



Universiteit
Leiden
The Netherlands

Quest for the cure: towards improving hematopoietic stem cell based lentiviral gene therapy

Tajer, S.P.

Citation

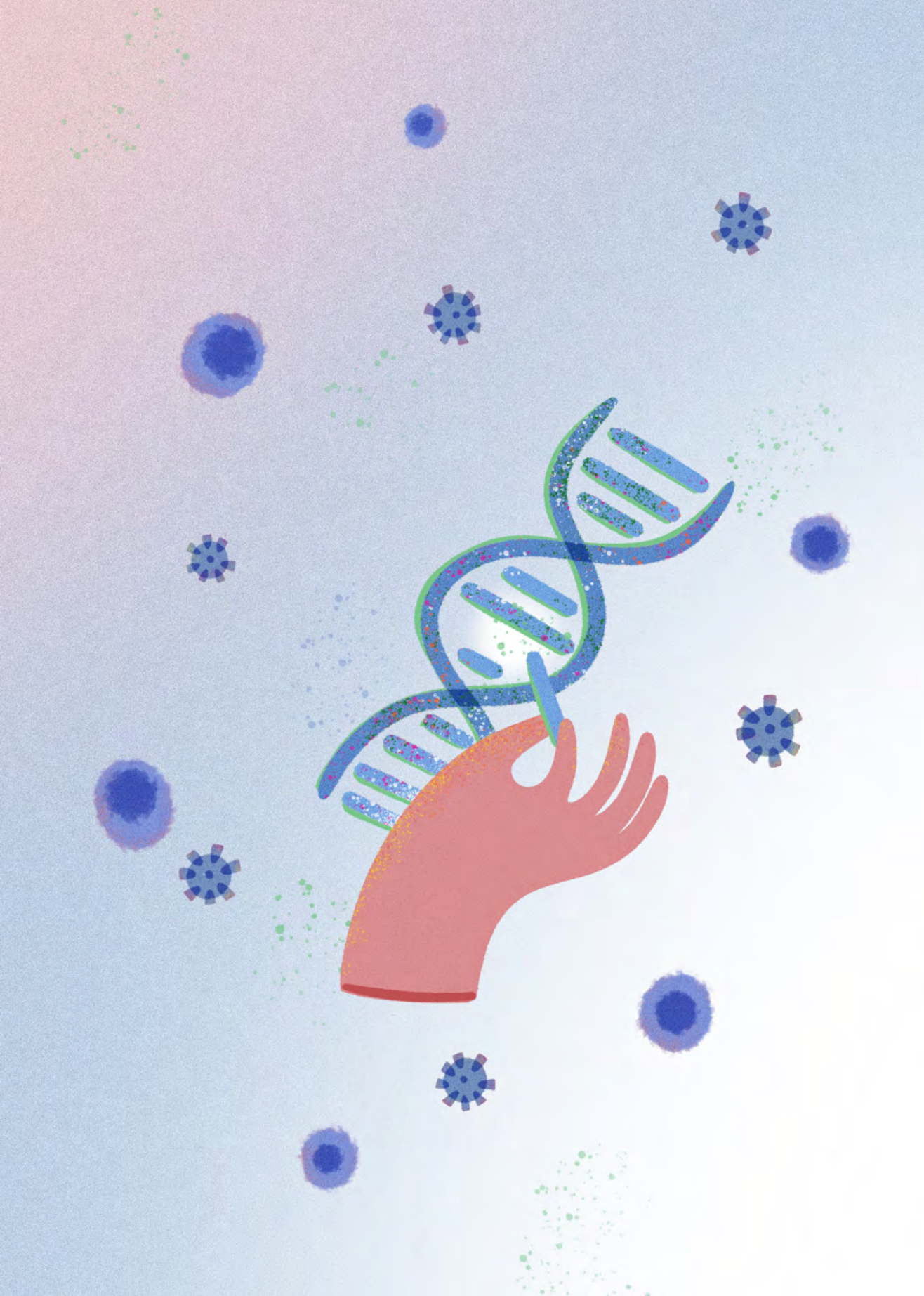
Tajer, S. P. (2024, December 17). *Quest for the cure: towards improving hematopoietic stem cell based lentiviral gene therapy*. Retrieved from <https://hdl.handle.net/1887/4172518>

Version: Publisher's Version

License: [Licence agreement concerning inclusion of doctoral thesis in the Institutional Repository of the University of Leiden](#)

Downloaded from: <https://hdl.handle.net/1887/4172518>

Note: To cite this publication please use the final published version (if applicable).



Chapter 4

Utilizing epigenetic regulators to improve HSC-based lentiviral gene therapy

*Parisa Tajer, Emin Onur Karakaslar, Kirsten Canté-Barrett, Brigitta A. E. Naber,
Sandra A Vloemans, Marja C.J.A van Eggermond, Marie-Louise van der Hoorn, Erik
van den Akker, Karin Pike-Overzet, Frank J. T. Staal*

Blood Advances, 2024

Abstract

Curative benefits of autologous and allogeneic transplantation of hematopoietic stem cells (HSCs) have been proven for various diseases. However, the low number of true HSCs that can be collected from patients and subsequently *in vitro* maintenance and expansion of true HSCs for genetic correction remain challenging. Addressing this issue, we here focused on optimizing culture conditions to improve the *ex vivo* expansion of true HSCs for gene therapy purposes. In particular, we explore the use of epigenetic regulators to enhance the effectiveness of HSC-based lentiviral (LV) gene therapy. The HDAC inhibitor Quisinostat and the bromodomain inhibitor CPI203 each promote *ex vivo* expansion of functional HSCs, as validated by xenotransplantation assays and single cell RNA-sequencing analysis. We confirmed the stealth effect of LV transduction on the loss of HSC numbers in commonly used culture protocols, while addition of Quisinostat or CPI203 improved expansion of HSCs in transduction protocols. Of note, we demonstrated that addition of Quisinostat improved LV transduction efficiency of HSCs and early progenitors. Our suggested culture conditions highlight the potential therapeutic effect of epigenetic regulators in hematopoietic stem cell biology and their clinical applications to advance HSC-based gene correction.

Introduction

Hematopoietic stem cells (HSCs) have been used successfully in allogeneic transplantation settings to treat hematological and immunological disorders, as they maintain homeostasis through their unique capacity of self-renewal and multipotency¹⁻³. Over the past two decades autologous HSC-based gene therapy has emerged as a compelling alternative to allogeneic transplantation as it is not dependent on finding a matched donor and avoids any risk of graft-versus-host disease. This has proven successful for several inherited diseases such as immune deficiencies, hematological disorders, but also metabolic diseases through *ex-vivo* manipulation of the patient's own HSPCs⁴⁻⁷. Lentiviral vectors (LVs) have emerged as vectors of choice in clinical settings for safer and more efficient transgene delivery to HSCs compared to γ -retroviral vectors that were used in initial gene therapy trials. Recently, gene editing has emerged as another powerful tool providing a platform for therapeutic correction of monogenic diseases. Proof of concept studies using CRISPR-Cas9 gene editing in hematopoietic stem and progenitor cells (HSPCs) have shown promise to treat hematological disorders⁸⁻¹⁰. Nevertheless, critical challenges such as the efficiency of targeting long-term HSCs, on- and off-target side effects and safety still need to be addressed.

For successful treatment outcome of hematological and immunological disorders, correction of long-term HSCs and progenitors is required to ensure long term correction of the disease¹¹. Both viral gene addition therapy as well as homology-directed recombination (HDR)-based gene editing approaches have shown preferential genetic correction of more proliferating progenitors, rather than quiescent HSCs *in vitro*, possibly due to better chromatin accessibility of relevant loci^{12,13}. Combinations of hematopoietic cytokines are commonly used in human HSC cultures to promote HSPC expansion for gene therapy purposes¹⁴. Although these cytokines support short-term maintenance of HSCs, they fail to expand functional HSCs, particularly in genetic manipulation settings.

Great effort has been put to develop culture conditions for HSC expansion *in vitro* by incorporation of small molecules such as UM171¹⁵, StemRegening-1¹⁶ or using chemically defined cytokine free medium¹⁷. Recent approaches of using various epigenetic regulators for HSC expansion *in vitro* have been reported. Epigenetic regulation is an essential intrinsic cue for normal haematopoiesis and cell fate decisions under physiological conditions¹⁸. Small molecules targeting chromatin

regulating proteins, such as histone deacetylase inhibitors (HDACi), DNA methylating agents, and Bromodomain and Extra-Terminal motif domain inhibitors (BETi) have been successfully used in culturing protocols of human HSCs¹⁹⁻²³. These findings have highlighted the importance of epigenetic regulators as a therapeutic target for HSC expansion and gene therapy purposes.

Methods

Human cells and CD34⁺ enrichment. Human cord blood was obtained after informed consent from Leiden University Medical Centre. Mononuclear Cells (MNCs) were obtained from cord blood by density centrifugation using Ficoll-Amidotrizaat. CD34⁺ cells were positively selected using the human CD34 UltraPure MicroBead Kit (Miltenyi Biotec) according to the manufacturer's protocol.

CD34⁺ cell culture. 100,000-250,000 enriched CD34⁺ cells/ml (>90% purity) were cultured in X-vivo15 medium (Lonza) supplemented with recombinant huSCF (300ng/ml), huTPO (100ng/ml), huFLT3 (100ng/ml) (Miltenyi Biotec), and small molecules of CPI203 (150nM) (Selleckchem) and Quisinostat (0.1, 0.5 and 1nM) (MedChemExpress) After 4-5 days of culture, expanded cells were harvested and counted using a nucleocounter 3000 (Chemometec) for subsequent immunophenotyping, transplantation in mice, and scRNA-seq.

Lentivirus production. HEK 293T cells were seeded at density of 4×10^6 cells in 10cm² plate. After 24 hours, cells were transfected using X-tremeGENE HP DNA transfection reagent (Sigma-Aldrich) at a mass ratio of 1:3 (DNA:X-tremeGene HP), with the plasmids. The amount of each viral component per million of cells was: 2.5 µg of pSIN.SF.EGFP.WPRE; 1.25 µg of pMDLg/pRRRE; 0.6 µg of pRSV-Rev; 0.75 µg of pMD2.VSVG. Supernatant was harvested, clarified with 0,45 µm filter (Whatman) at 24h and 48h post transfection. Supernatant from different time points were pooled together. Virus concentration was performed using Vivaspin20 (Sartorius) according to the manufacturer's instruction.

Lentivirus transduction. One day prior to transduction, CD34⁺ cells were cultured in cytokine supplemented X-vivo15 medium in combination with CPI203 (150nM) or Quisinostat (0,5nM). After overnight stimulation, lentiviral particles carrying GFP transgene were added to the cells at MOI of 1.5 as well as Lentiboost (Sirion) final concentration of 1ug/ml followed by spinoculation at 32 °C for 1 hour at 800g. Four

days post-transduction, transduced cells were used for *in vitro* and *in vivo* approaches.

Determination of vector copy number (VCN) by RT-qPCR. Quantitative (q)PCR was used for the quantitative analysis of proviral DNA copies in transduced cells using Hiv-psi and Albumine as housekeeping gene. Genomic DNA of transduced cells was extracted using GeneElute Mammalian Genomic DNA kit (Sigma-Aldrich). qPCR was performed using TaqMan Universal Master Mix II (ThermoFisher) in combination of specific probes from universal library (Roche) on the Quantstudio system (Thermo Fisher Scientific).

Mice. NOD.Cg-Prkdcscid Il2rgtm1Wjl/SzJ (NSG) mice were purchased from Charles River (France). All animal experiments were approved by the Dutch Central Commission for Animal experimentation (Centrale Commissie Dierproeven, CCD).

Primary and secondary transplantations into NSG mice. For the primary transplantations, *ex vivo* expanded CD34⁺ cells (25,000 or 50,000 total nucleated cells per mouse) in Iscove's Modified Dulbecco's Medium (IMDM) without phenol red (Gibco) were transplanted by tail vein injection into pre-conditioned recipient NSG mice (n=5). For the secondary transplantations, bone marrow (BM) cells from primary recipient mice from each group were pooled and 1/7th of the pooled cells were injected into pre-conditioned secondary recipient NSG mice (n=5). 6-8-week-old recipient mice were conditioned with two consecutive doses of 25 mg/kg Busulfan (Sigma-Aldrich) (48h and 24h prior transplantation). Mice used for transplantation were kept under specific pathogen-free conditions. The first four weeks after transplantation mice were fed with additional DietGel recovery food (Clear H₂O) and antibiotic water containing 0.07 mg/mL Polymixin B (Bupha), 0.0875 mg/mL Ciprofloxacin (Bayer b.v.). Peripheral blood (PB) from the mice was drawn by tail vein puncture every 4 weeks until the end of the experiment. At the end of the experiment, PB, thymus, spleen and BM were harvested. Mice were euthanized via CO₂-asphyxiation.

Flow cytometry. *Ex vivo* cultured cells were stained with the live/dead marker Zombie (Biolegend) according to the manufacturer's instruction. Subsequently, cells were stained with antibodies listed in Supplementary Table 1, and incubated for 30 min at 4°C in the dark in FACS Buffer (PBS pH 7.4, 0.1% azide, 0.2% BSA). Single cell

suspensions from murine BM, thymus and spleen were prepared by squeezing the organs through a 70 μ M cell strainer (BD Falcon). Erythrocytes from PB and spleen were lysed in NH_4Cl (8,4 g/L)/ KHCO_3 (1 g/L). Single cell suspensions were counted and stained as described above. When 7AAD and KI67 staining was needed, intracellular staining was performed using the Transcription Factor Staining Buffer Set (eBioscience), according to manufacturer's instruction. All cells were measured on an Aurora spectral flow cytometer (Cytek). The data was analysed using FlowJo software (Tree Star).

Single cell analysis quality control (QC) pipeline. QC and downstream analyses of scRNA-seq data were performed using Seurat version4 ²⁴. The quality control pipeline before integration consists of three steps per sample: 1) soft filtering, 2) removal of low-quality cluster, and 3) doublet detection. In soft filtering, Seurat objects were created with cells expressing at least 200 genes and with the genes expressed at least in 3 cells. Then, standard Seurat command list was run to detect low quality clusters. We removed a cluster only if it had higher than 15% mitochondrial and less than 1000 mRNA in median. Next, we ran DoubletFinder v3 per sample with 7.5% detection rate and filtered for the singlets ²⁵. To integrate the samples, CCA mode of Seurat pipeline was used with most variable 2000 features. Finally, after integration we filtered cells with higher than 15% mitochondrial mRNA.

Cell type predictions for stimulated cells. After QC, we subsisted the unstimulated CD34^+ cells (n=13,429). Then, these cells were clustered again with a higher resolution parameter (resolution=1.2) to ensure precise annotation in down-stream projections of stimulated samples. Furthermore, we checked cluster stability with *clustree* R package ³¹. To annotate each cell cluster, we used a combination of cord blood markers from Dong *et al* ³² and differentially expressed genes (DEGs). Top 20 DEGs per cell cluster from unstimulated cells are provided in Supplementary Table 2. To project these annotations onto stimulated samples, we trained a random forest model with 300 trees using unstimulated CD34^+ cells via 2000 integrated features. Cross-validation on out-of-bag data showed that HSCs could be predicted with an accuracy of 81.2%.

Differential expression and gene set enrichment analysis. Differential expression analysis was conducted with MAST ³³ with a cut-off of at least 25% difference in cells expressing a given gene. Then, clusterprofiler ³⁴ was used along with biological

processes subset of GO terms for gene set enrichment analysis. Pathway p-values are adjusted with Benjamini-Hochberg procedure. Pathways enriched with adjusted $p < 0.05$ are selected. ggplot2 library was used for all visualizations unless indicated otherwise.

Statistics. Statistics were calculated and graphs were generated using GraphPad Prism9 (GraphPad Software). Statistical significance was determined by standard two-tailed Mann-Whitney U tests, unpaired t-tests and ANOVA tests ($*p < 0.05$, $**p < 0.01$, $***p < 0.001$ and $****p < 0.0001$).

Data sharing statement. For original data, please contact f.j.t.staal@lumc.nl. The sequencing data reported in this article have been submitted to the European Genome Phenome Archive with accession numbers of EGAD50000000254.

Results

CPI203 and Quisinostat support expansion of phenotypic HSCs *in vitro*

In a clinical gene therapy setting, HSPCs often are cultured in serum free medium supplemented with the essential cytokines stem cell factor (SCF), thrombopoietin (TPO), Fms-like tyrosine kinase 3 (FLT3) and Interleukin-3 (IL3)⁵. We have previously showed the adverse effect of IL3 on *ex vivo* HSC expansion and subsequently low engraftment in mice, suggesting exclusion of IL3 from culture protocols¹⁴. CD34⁺ cells from cord blood were expanded for 4 days in a cytokine cocktail of SCF, TPO and FLT3 (called STF), with or without addition of Quisinostat (STF+Q) or CPI203 (STF+CPI203) (Figure 1A). Flow cytometry analysis showed that addition of Quisinostat increased the expression of the HSC markers CD34, CD90, and CD201, while low expression of CD38 and CD45RA were maintained in presence of both CPI203 and Quisinostat (Figure 1B). This resulted in substantial increase of the frequency and count of CD34⁺CD38^{-/lo}CD90⁺CD45RA⁻CD201⁺ phenotypic HSCs (Figure 1C-D); in contrast, STF cytokine cocktail supported expansion of multipotent progenitors (MPPs) and different lineage progenitors after four days (Figure 1D-E). Both HDAC and BET inhibitors have been clinically evaluated as antitumor agents, mainly due to their antiproliferative effect on cancer cells by inducing G0/G1 cycle arrest through P13K-AKT pathway³⁵ and targeting *MYC*, respectively³⁶. In this study, increasing concentrations of Quisinostat reduced the total nucleated count (TNC) but increased the frequency of phenotypic HSCs (Supplementary Figure 1B-C). Addition of CPI203 reduced total cell counts and CD34⁺ numbers after four days of

culture (Supplementary Figure 1D). This is consistent with the observed significant increase of G0 frequency and a decrease of proliferative states of S_G2 in HSCs, whereas no changes in cell cycle states were observed in the Quisinostat-treated HSCs (Figure 1F).

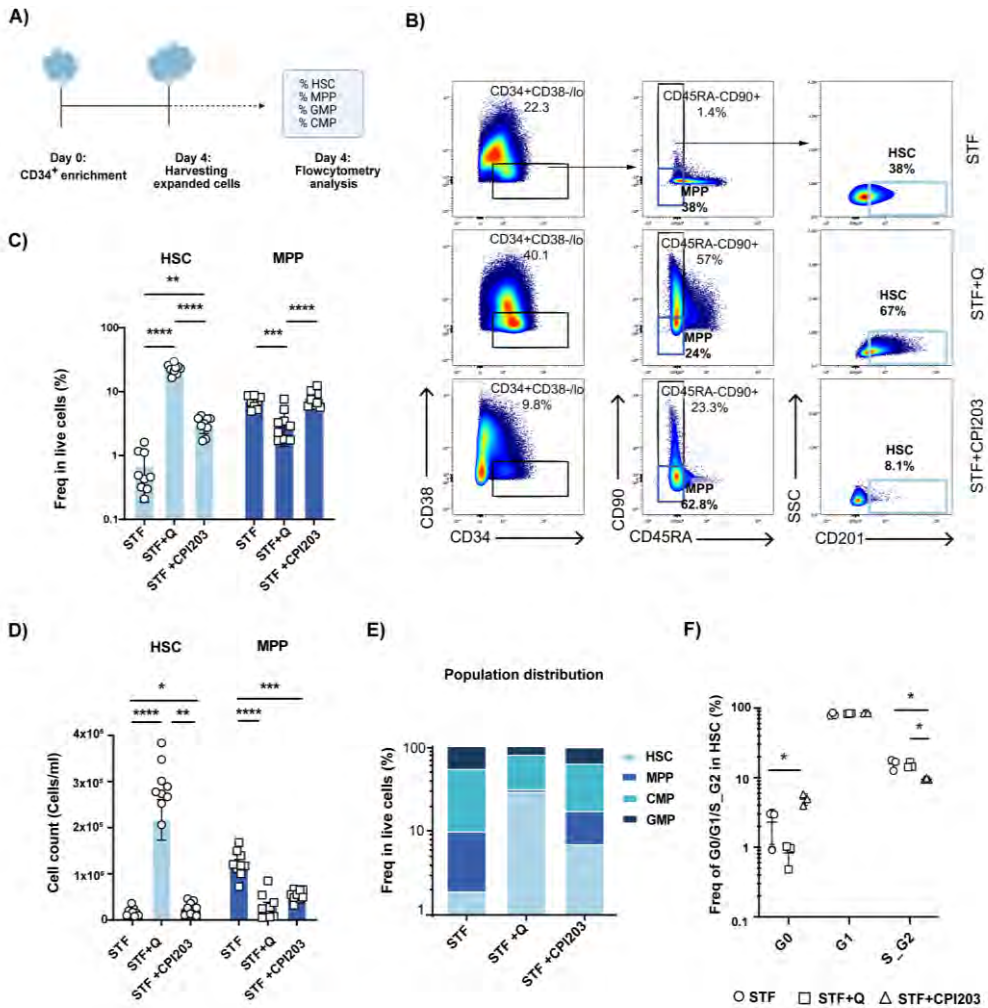


Figure 1. CPI203 and Quisinostat support ex vivo expansion of HSCs. A) Schematic experimental design. CD34⁺ cells were enriched from cord blood (CB) and cultured in cytokine supplemented medium with Quisinostat (0,5nM) or CPI203 (150nM) for 4 days. B) Representative gating strategy of expanded HSCs (CD34⁺ CD38⁻ CD90⁺ CD45RA⁻ CD201⁺) and MPPs (CD34⁺CD38⁻CD90⁻CD45RA⁺) in indicated culture condition. C) The graph indicates frequency of HSC and MPP after 4 days of culture in the indicated culture condition (n=9, Mean±SD). D)

HSC and MPP count after 4 days of culture in the indicated culture condition (n=9, Mean±SD). E) Stacked bar plot shows composition of HSPCs expanded with only cytokines and in presence of Quisinostat and CPI203. F) Frequency of cell cycle stages in expanded HSCs (n=3, Mean±SD). Statistical significance was determined by two-way anova test for multiple comparison *p<0,05, **p<0,01 and ***p<0,001, ****p<0,0001.

Quisinostat increases LV transduction efficiency *In vitro*

LV-based gene therapy in HSCs has proven to be safe and effective for correction of different blood disorders. Nevertheless, often clinical applications are limited by suboptimal transduction efficiency especially in true HSCs, due to their dormant state.¹¹. Various transduction protocols containing small molecules such as Prostaglandin E₂³², Cyclosporin H¹² and poloxamer F108 (LentiBOOST)³³ have been reported to improve transduction efficiency *in vitro* and *in vivo*.

To assess the efficiency of our suggested HSC expansion culture conditions for LV based gene therapy settings, CD34⁺ were transduced with LV carrying green fluorescent protein (GFP), in presence of either CPI203 or Quisinostat (Figure 2A). Both flow cytometry and vector copy number analyses showed that addition of Quisinostat in culture increased the LV transduction efficiency significantly in total cells (Figure 2B-C, Supplementary Figure 2A). Notably, Quisinostat has more than doubled the transduction efficiency in HSCs (Figure 2D-E) and other progenitors in comparison with other culture conditions (Supplementary Figure 2B).

HDACis impact gene expression status, by increasing acetylation level, leading to more transcriptionally active and accessible chromatin. Upon the introduction of Quisinostat, we have confirmed that the acetylation level of lysine 27 on Histone 3 (H3K27) in CD34⁺, HSCs, and MPPs has significantly increased (Figure 2F). This finding provides a potential explanation for the observed enhanced transduction efficiency.

***In vivo* repopulating potential of transduced HSPCs from an optimized cell culture**

To evaluate the repopulation potential and *in vivo* engraftment capabilities of cultured HSPCs, we performed xenotransplantation assays, which are the accepted gold standard for assessing multilineage potential and self-renewal of human HSCs, as reliable *in vitro* assays to address stem cell functionality are currently absent³⁴.

We transplanted 5x10⁴ and 2,5x10⁴ expanded cells from the conditions 'STF', 'STF+CPI203' and 'STF+Q' into recipient NSG mice (Figure 3A). All mice (5 out of 5) injected with Quisinostat- and CPI203-expanded cells showed signs of human engraftment (≥ 0.1% of huCD45⁺) at both cell doses, whereas mice that received

cells expanded in cytokine cocktail only showed consistent engraftment solely at higher cell doses. Significantly higher human chimerism (huCD45⁺) in BM was detected in Quisinostat and CPI203 culture groups when mice received lower cell dose (Figure 3B-C). Given this difference, the subsequent sections will primarily focus on the results from mice receiving the lower cell dose of 25,000 cells. Peripheral blood analysis over time showed higher human chimerism in mice receiving CPI203-cultured cells (Figure 3D). Interestingly, transplantation of CPI203-expanded cells also resulted in substantial increased engraftment in the thymus (Thy), whereas no differences were observed in the spleen (Sp) (Figure 3E). The frequency of human CD34⁺ was significantly higher in BM in the CPI203-expanded culture group (Figure 3F). Distinct multilineage output in different organs demonstrated that both Quisinostat and CPI203 cultured cells yielded improved lymphoid development in BM, with significantly higher frequency of CD19⁺, common lymphoid progenitors (CLPs) and Pro-B cells (Figure 3F). Strikingly, cells expanded with CPI203 exhibited enhanced engraftment in thymus comparing to other organs (Supplementary Figure 3 A), accompanied by an increased frequency of CD3⁺, CD4⁺CD8⁺, and TCRab⁺ cells (Figure 3G).

Subsequently, we examined the frequency of transduced cells (% GFP⁺) in engrafted cells in the BM (Figure 4A). In alignment with our *in vitro* results, mice that received Quisinostat-expanded cells, exhibited a greater frequency of transduced huCD45⁺ in BM, PB and spleen, with a marginal increase observed in thymus when compared to other culture conditions (Figure 4B). Further analysis has also revealed higher transduction efficiency across various lineages in BM (Figure 4C). Secondary transplantation was performed to confirm long-term repopulation capacity of expanded cells in BM (Figure 4D-E), and engraftment of transduced cells in BM (Figure 4F). The data confirm that addition of CPI203 or Quisinostat maintain HSC self-renewal.

scRNA-seq reveals epigenetic regulators support expansion of HSCs upon LV transduction

To reveal cellular heterogeneity within CD34⁺ cells among different culture conditions, we performed single cell RNA-sequencing (scRNA-seq). Specifically, we set out to compare our culture conditions as well as the effect of LV transduction on the cellular composition of the total CD34⁺ cells.

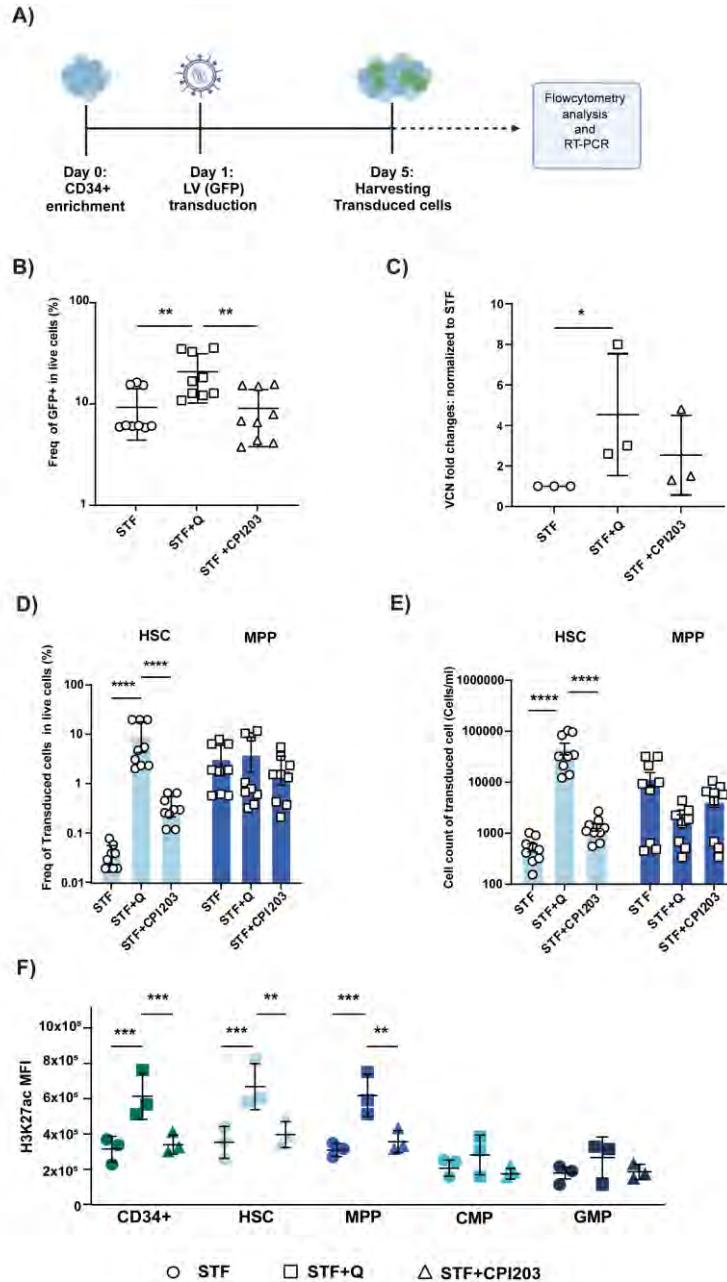


Figure 2. Quisinostat increases LV transduction efficiency. A) Schematic experimental design. CD34⁺ cells were transduced with LV-GFP, 24h after stimulation in either only cytokine supplemented medium or in presence of Quisinostat (0,5nM) or CPI203 (150nM). Cells were harvested for flow cytometry analysis and DNA isolation and RT-PCR, 4 days after transduction. B) Frequency of GFP⁺ 4 days after transduction in live cells (n=9, Mean±SD). C) Vector copy number (VCN) was determined using RT-PCR (n=3, Mean±SD, *p<0,05, unpaired t-test).

D) Frequency of transduced HSCs and MPPs in indicated culture conditions are shown (n=9, Mean±SD). E) Cell count of transduced HSCs and MPPs (n=9, Mean±SD). F) The plot shows the mean fluorescent intensity (MFI) of H3K27ac in different population of expanded cells in indicated culture conditions (n=3, Mean±SD). Statistical significance was determined by two-way anova test with multiple comparison *p<0,05, **p<0,01 and ***p<0,001, ****p<0,0001.

Enriched CD34⁺ cells (hereafter referred to as unstimulated CD34⁺) were used as a reference control, along with six samples that were cultured and transduced in medium supplemented with cytokines alone, Quisinostat or CPI203 (Figure 5A). After manual annotation of unstimulated CD34⁺ cells into multiple different progenitor cell types based on gene expression profiles, all samples were integrated and analyzed using Seurat. We identified 13 major clusters (Figure 5B-C) corresponding to several well recognized early differentiation stages of CD34⁺ cells. Based on the marker genes adopted from *Dong et al*²⁷, and top differential expressed genes (DEGs) (Supplementary Table 2), we identified the *bona fide* HSC population as having high expression of *AVP* and *HLF* genes, while lacking lineage specific genes such as *MPO*, *DUTT*, *GATA2*. The populations with lower expression of *HLF* and *AVP* were identified as MPP, as they have been proposed to be early progenitors¹⁷. Furthermore, progenitors of distinct lineages of myeloid, lymphoid, erythroid (Eryth) and megakaryocytic cells (Mks) were identified using their unique gene signatures (Figure 5C and Supplementary Figure 4A).

Comparing HSPC composition among different culture conditions, a higher frequency of HSCs was observed in culture conditions with CPI203 and Quisinostat compared to the STF condition (Figure 5 D-E, and Supplementary Figure 4D). In cultures supplemented with Quisinostat and CPI203, expression of HSC signature genes of *HLF*, *RORA* and *HOXA9* was higher compared to cytokine-only (STF) expanded cells, while *AVP* gene expression decreased in CPI203 expanded cells (Supplementary Figure 4C). Moreover, consistent with our flow cytometry analysis (Figure 1B), Single cell transcriptomics data confirmed higher expression of *CD34*, *THY1* and *PROCR* genes in Quisinostat-expanded cells, while expression of *CD38* gene was decreased (Figure 5F).

In accordance with our *in vivo* results, the scRNA-seq data also demonstrated the increase in frequencies of lymphoid multipotent progenitors (LMPPs), B cells, common myeloid progenitors (CMPs) and Mks in CPI203 expanded cells (Figure 5E, and Supplementary Figure 4D). Collectively, our *in vivo* and *in vitro* results suggest

that addition of CPI203 in HSC expansion protocol not only has improved *ex vivo* expansion of HSCs, but has also supported the priming of cells towards the lymphoid lineage. On the other hand, the addition of Quisinostat reduced the frequency of granulocyte monocyte progenitors (GMPs), while increasing erythroid progenitors (MEPs) and myeloid progenitors (CMPs) (Figure 5E, and Supplementary Figure 4D).

Of note, our data showed higher frequency of MEPs, Eryth and Mks upon LV transduction, suggesting LVs could skew cells towards the erythroid lineage in culture conditions containing Quisinostat or CPI203. In contrast, higher frequency of myeloid-lymphoid progenitors (MLPs) have been detected in cytokine-expanded cells (Supplementary Figure 4D). This possible lineage skewing upon LV transduction warrants further investigation.

Finally, single cell transcriptomics results showed LV transduction in itself induces cell proliferation (Supplementary Figure 4B) but reduces the frequency of the HSC population compared to non-transduced conditions. This decrease is more prominent in STF condition, while inclusion of Quisinostat and CPI203 in the LV transduction protocol has helped to maintain HSCs (Figure 5D, and Supplementary Figure 4D). LV transduction induces innate immune response via indirect activation of interferon (IFN) responses through different pathways such as Toll-like receptors (TLRs)³⁵, DNA damage response³⁶ or DNA sensor responses³⁷. We have detected elevated gene expression related to the interferon response and DNA damage response, such as *TP53*, *IFITM2*, *IFITM3*, *IFI16*, *TMEM173*, *DDB2* in expanded cells. However, addition of CPI203 results in a reduction of their expression. Additionally, no changes in expression of TLRs was observed (Supplementary Figure 4E). Using Gene set enrichment analysis and checking the cellular processes associated with the differentially expressed genes (Figure 5G), we noted that the addition of Quisinostat to the LV transduction condition, resulted in differential expression of genes associated with DNA replication and chromosome organization, in line with the functional effects observed.

Collectively, these findings indicate that addition of Quisinostat and CPI203 enhances the expansion of hematopoietic stem cells (HSCs) while simultaneously priming cells for erythroid and lymphoid lineages, respectively. Furthermore, our study highlights the impact of lentiviral (LV) transduction on cellular heterogeneity, revealing a significant loss of HSCs with the commonly employed protocol in clinical settings.

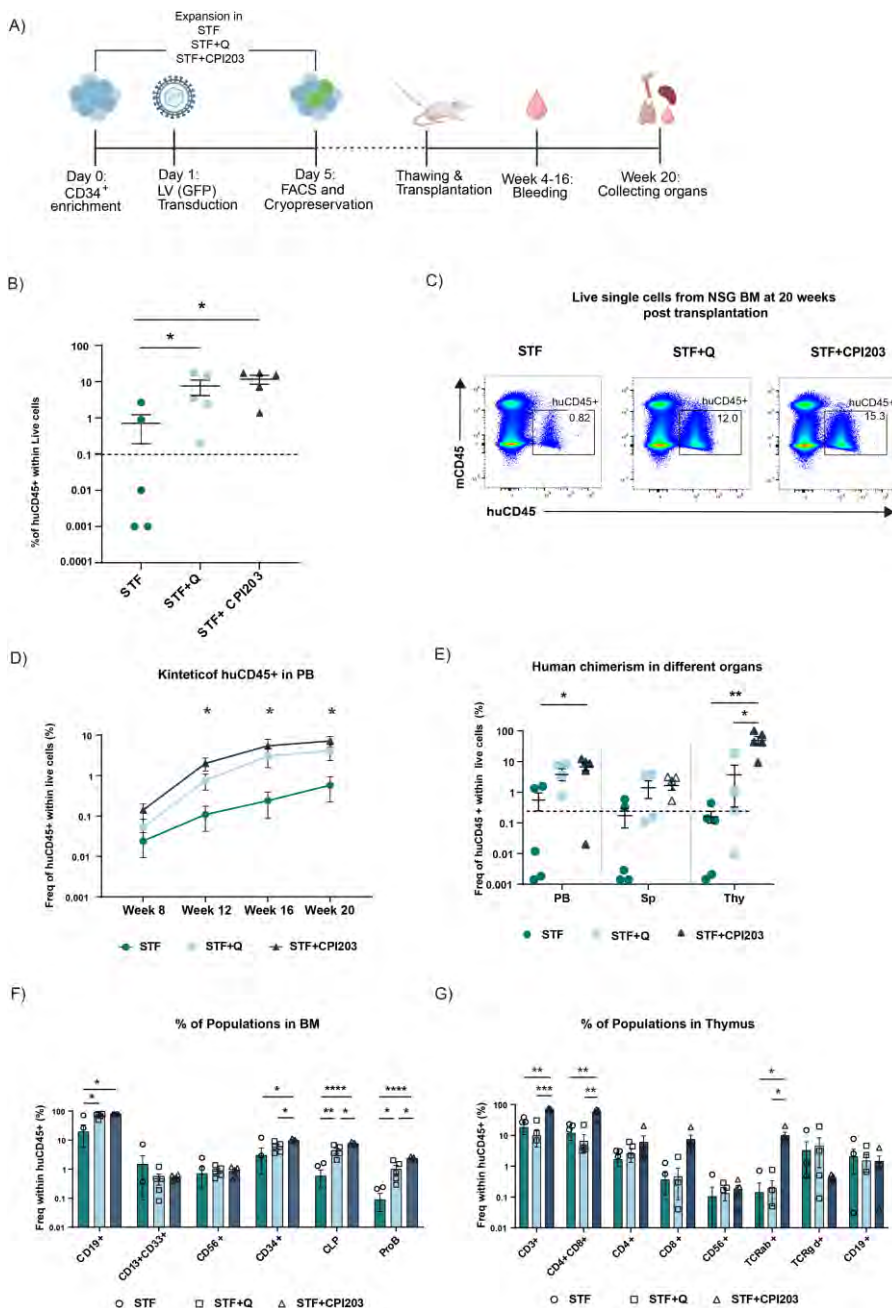


Figure 3. CPI203 and Quisinstat support expansion of functional HSCs. A) Schematic overview of primary transplantation. 25,000 and 50,000 total nucleated expanded cells in indicated culture conditions were transplanted per mouse. B) Human engraftment in Bone Marrow (BM) of NSG mice at week 20 post transplantation (n=5 mice per group, Mean±SEM, *p<0,05, Statical significance was calculated by one-way anova, with multiple comparison). C) Representative FACS plots of human CD45 in NSG BM at week 20 post transplantation. D)

Kinetics of chimerism in Peripheral Blood (PB) over time (n=5 mice per group, significant of STF vs STF+CPI203 is shown in the plot). E) Human engraftment in different organs (SP=Spleen, Thy= thymus) at week 20 post transplantation (n=5 mice per group). F) Frequency of different populations in BM (n=5 mice per group). G) Frequency of different populations in thymus (n=5 mice per group, Mean±SEM). Statistical significance was calculated by two-way anova with multiple comparison *p<0.05, **p<0.01, ***p<0.001, ****p<0.0001.

Discussion

Working towards improving HSC expansion protocols for gene therapy purposes, in this study we have evaluated existing and newly tested culture conditions for HSC expansion and gene modification. We incorporated the small molecules CPI203—a BETi that has been previously reported by Hua *et al*¹⁹—and the HDACi Quisinostat for testing *ex vivo* expansion of HSCs and their genetic modification. BET proteins interact with acetylated lysins at transcriptional start sites that regulate transcription through RNA polymerase II complex formation. BETi regulates transcription by blocking BET protein binding to histones. Therapeutic benefits of BETis have been investigated in several cancer trials, however, their clinical progression has been challenging and none have received regulatory approval³⁸. On the other hand, Quisinostat, an HDACi targeting HDAC I and II, has been evaluated in several clinical trials for different malignancies³⁹⁻⁴¹. Recent research suggests Quisinostat inhibits the cancer cell self-renewal by re-establishing expression of histone linker H1.0⁴². H1 is highly conserved and involved in embryonic stem cell differentiation and mammalian development, although the role of H1 linker in HSCs development and fate decisions needs further investigation.

We have reported improved culture conditions for *ex vivo* expansion of true HSCs, which could be implemented in lentiviral transduction protocols for gene therapy purposes. We showed that the inclusion of epigenetic regulators of Quisinostat and CPI203 increased expansion of HSCs. In addition, the positive effect of Quisinostat on transduction efficiency provides a major benefit for the gene therapy field. This not only ensures long-term correction of true HSCs, which is the ultimate goal of gene therapy, but also reduces the costs associated with viral vectors, since less lentiviral virus would be required to achieve a desired vector copy number.

Importantly, our scRNA-seq data reveals the stealth effect of LV transduction on loss of HSCs, particularly in the conventional clinical protocol of STF-cytokine-expanded cells. LV transduction induces an innate immune response via indirect activation of interferon (IFN) responses through different pathways such as Toll-like receptors (TLRs)³⁵, DNA damage response³⁶ or DNA sensor responses³⁷. Even though LVs can escape the innate immune responses⁴³, they can be detected through TLRs³⁵ in

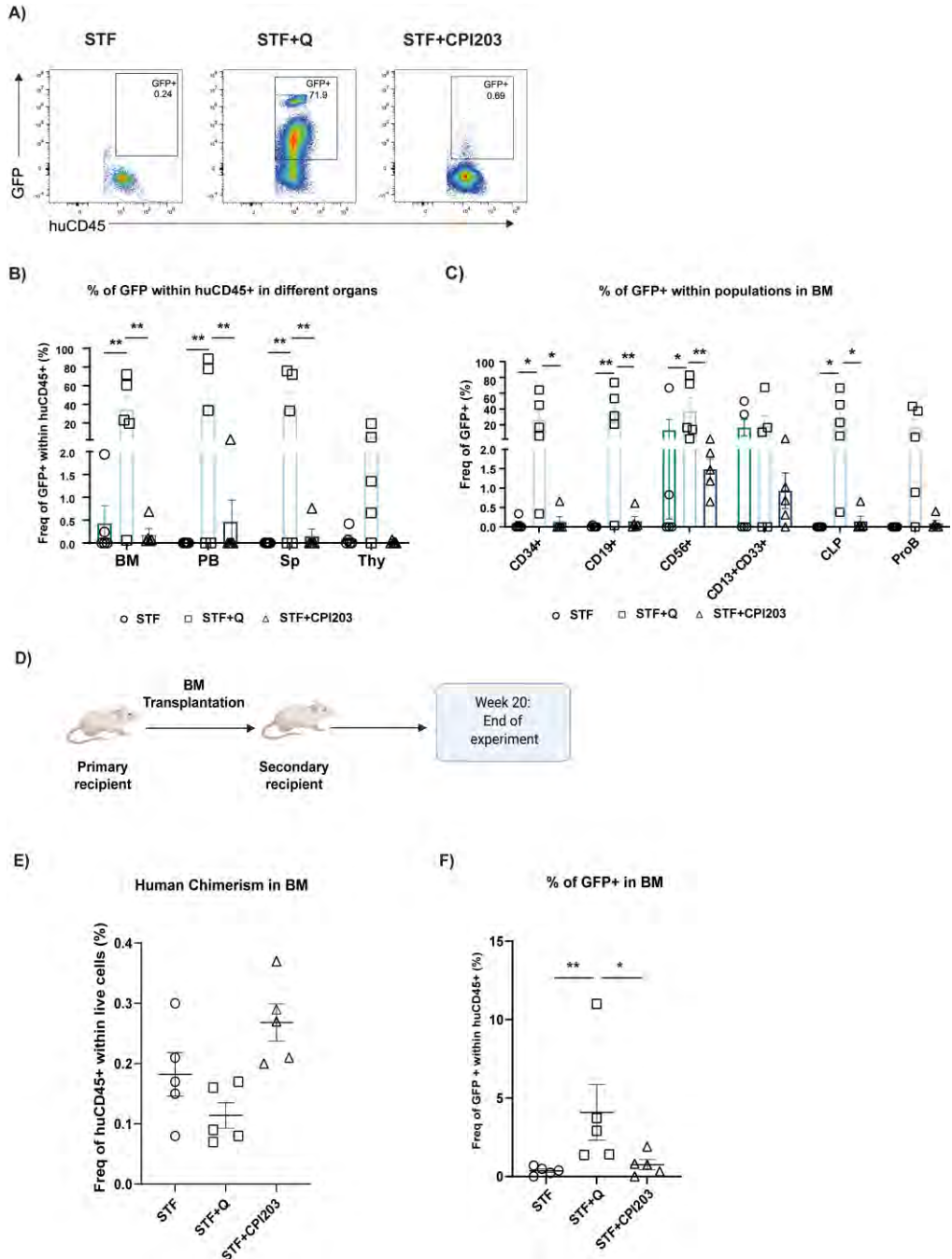


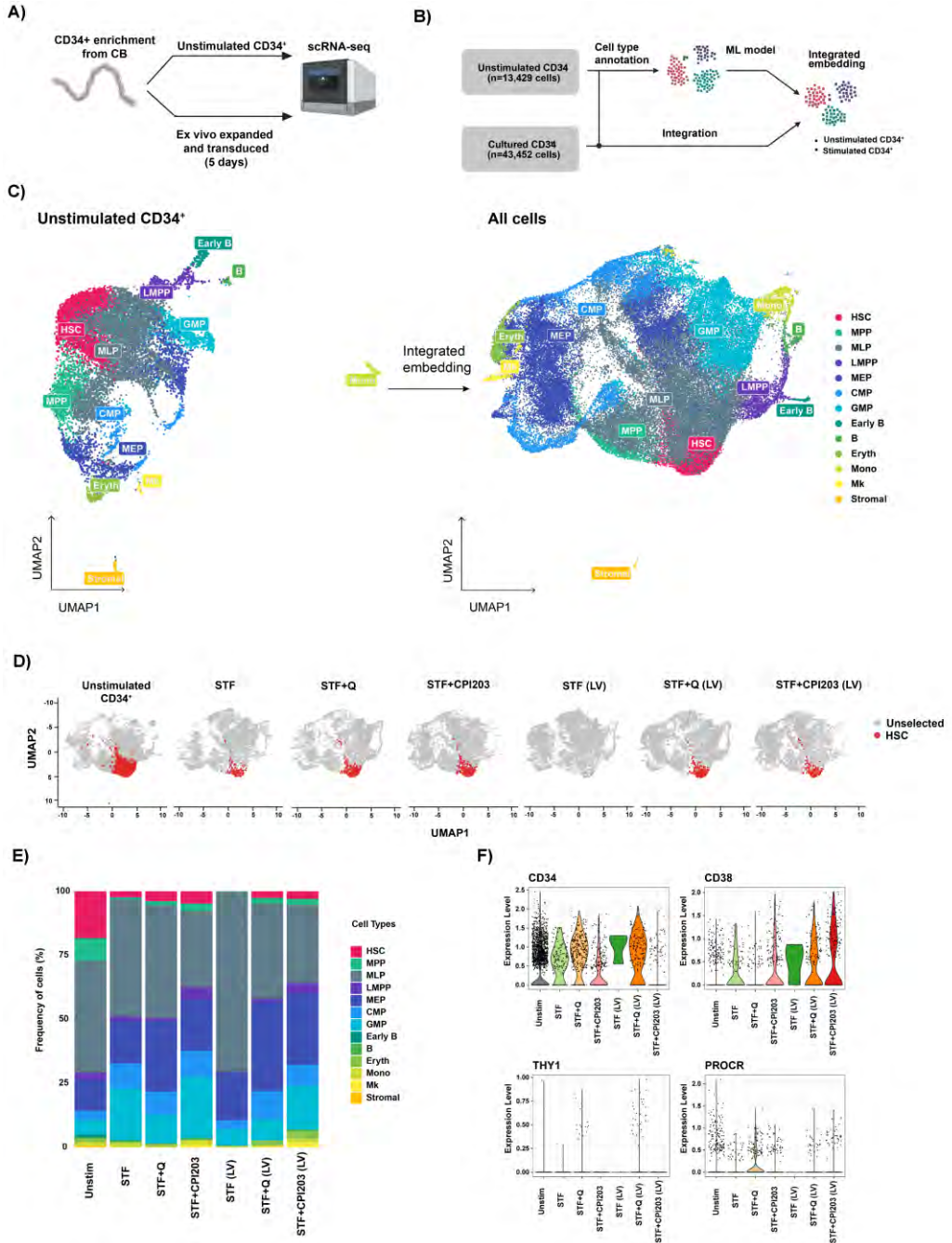
Figure 4. Quisinstat supports better engraftment of transduced cells in vivo. A) Representative FACS plots of BM at week 20 post transplantation in primary mice. B) Frequency of GFP⁺ cells in different organs (n=5 mice per group, Mean±SEM, **p<0,01. Statistical significance was calculated by two-way anova, multiple comparison). C) Frequency of transduced populations

within huCD45⁺ in BM at 20-week post transplantation in primary NSG mice (n=5 mice per group, Mean±SEM, *p<0,05, **p<0,01, Statistical significance was calculated by two-way anova, multiple comparison). D) Schematic design of secondary transplantation into NSG mice. E) Human chimerism in BM at week 20 post transplantation (n=5 mice per group, Mean±SEM. Statical significance was calculated by Mann-Whitney test). F) Frequency of transduced cells (GFP⁺) in BM (n=5 mice per group, Mean±SEM, *p<0,05, **<0,01. Statical significance was calculated Mann-Whitney test).

HSPCs or trigger p53 signaling followed by robust induction of IFN responses ⁴³. Human CD34⁺ cells express *TLR3*, *TLR4*, *TLR7*, *TLR8* and *TLR9* to detect infection and induce innate immune response immediately ³⁵. Upon viral infection under physiological conditions, IFN- α induction leads to proliferation as a response to clear infections ⁴⁴. In addition, results from mouse studies showed induction of IFN- γ impairs HSC self-renewal and restore of HSCs number upon viral infection ⁴⁵. However, in our study no changes in *TLRs*' gene expressions were found. Strikingly, the benefit of CPI203 in gene editing can be investigated as it reduces interferon responses through p53 and reduced DNA damage responses.

Furthermore, our *in vivo* study suggests that CPI203 improved lymphoid development in BM and significantly in thymus without compromising other lineages, a benefit that would be valuable for patients with an impaired immune system. Moreover, based on our scRNA seq data, Quisinostat primed HSCs toward the erythroid lineage, which also can hold promises for gene therapy targeting blood disorders.

In the realm of clinical trials focused on HSC-based gene therapy, substantial financial investments are dedicated to producing Good Manufacturing Practice (GMP) grade LV batches. Frequently, the expenses associated with generating these batches reach into the millions of dollars, even for a small number of patients. Compliance with regulatory standards mandates full-scale test runs in meticulously controlled clean room environments. Consequently, the limited availability of GMP-grade virus for patient treatment significantly amplifies the overall costs associated with gene therapy medicines, emerging as a critical concern within the field ⁴⁶. This underscores the pressing need for advancements in HSC transduction protocols to alleviate the financial burden and streamline the production of gene therapies. Here we have reported on enhanced culture conditions that not only improve transduction efficiency but also preserve the integrity of HSCs. Such optimization is imperative for achieving a more favorable clinical outcome and emphasizes the importance of refining current protocols for expanded hematopoietic cell therapies.



G)

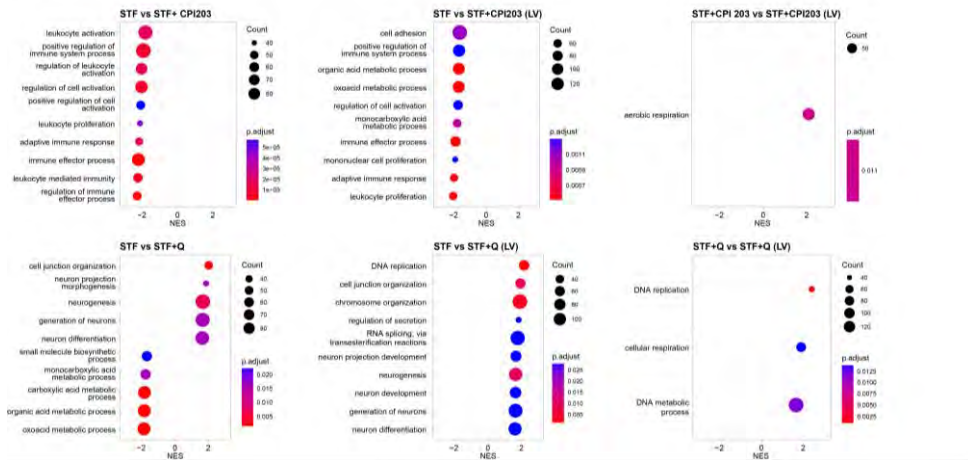


Figure 5 (continued). Single cell transcriptome analysis reveals *Quisinosat* and *CPI203* maintain HSCs upon LV transduction in *CD34⁺*. A) Schematic experimental design. B) Mock-up schematic of cell type projection. C) UMAP plots of unstimulated *CD34⁺*, and integrated UMAP of all conditions D) UMAP displaying HSCs per each condition. E) Bar plot represents population distribution. F) Violin plots displaying expression level of selected HSC surface marker genes in indicated condition.

Acknowledgment

This work was supported in part by an unrestricted educational grant from Batavia Biosciences (PT). Work in the Staal laboratory is supported in part by a ZonMW E-RARE grant (40-419000-98-236 020) and EU H2020 grant RECOMB (755170-2) and has received funding from the European Union Horizon 2020 research and innovation program as well as from reNEW, the Novo Nordisk Foundation for Stem Cell Research (*NNF21CC0073729*).

Authorship

P.T designed, performed, analyzed experiments, and wrote the manuscript; E.O.K performed bioinformatic analysis; K.C.B supported *in vivo* experiments. B.A.E.N, S.A.V and M.C.J.A.s.E assisted with mouse experiments. M.L.H provided cord blood for this study. E.V.D.A supported with scRNA seq experimental design; K.P.O and F.J.T.S provided supervision and revision of the manuscript. All authors have read and agreed to the final version of manuscript.

References

1. Seita J, Weissman IL. Hematopoietic stem cell: self-renewal versus differentiation. *Wiley Interdiscip Rev Syst Biol Med*. Nov-Dec 2010;2(6):640-53. doi:10.1002/wsbm.86
2. Weissman IL, Shizuru JA. The origins of the identification and isolation of hematopoietic stem cells, and their capability to induce donor-specific transplantation tolerance and treat autoimmune diseases. *Blood*. Nov 1 2008;112(9):3543-53. doi:10.1182/blood-2008-08-078220
3. Eaves CJ. Hematopoietic stem cells: concepts, definitions, and the new reality. *Blood*. 2015;125(17):2605-2613. doi:10.1182/blood-2014-12-570200
4. Cavazzana-Calvo M, Hacein-Bey S, de Saint Basile G, et al. Gene therapy of human severe combined immunodeficiency (SCID)-X1 disease. *Science*. Apr 28 2000;288(5466):669-72. doi:10.1126/science.288.5466.669
5. Garcia-Perez L, van Eggermond M, van Roon L, et al. Successful Preclinical Development of Gene Therapy for Recombinase-Activating Gene-1-Deficient SCID. *Mol Ther Methods Clin Dev*. Jun 12 2020;17:666-682. doi:10.1016/j.omtm.2020.03.016
6. Eichler F, Duncan C, Musolino PL, et al. Hematopoietic Stem-Cell Gene Therapy for Cerebral Adrenoleukodystrophy. *New England Journal of Medicine*. 2017;377(17):1630-1638. doi:10.1056/NEJMoa1700554
7. Ribeil J-A, Hacein-Bey-Abina S, Payen E, et al. Gene Therapy in a Patient with Sickle Cell Disease. *New England Journal of Medicine*. 2017;376(9):848-855. doi:10.1056/NEJMoa1609677
8. Gene Editing for the Treatment of Primary Immunodeficiency Diseases. *Human Gene Therapy*. 2021;32(1-2):43-51. doi:10.1089/hum.2020.185
9. Rai R, Romito M, Rivers E, et al. Targeted gene correction of human hematopoietic stem cells for the treatment of Wiskott -Aldrich Syndrome. *Nat Commun*. Aug 12 2020;11(1):4034. doi:10.1038/s41467-020-17626-2
10. Frangoul H, Altshuler D, Cappellini MD, et al. CRISPR-Cas9 Gene Editing for Sickle Cell Disease and β -Thalassemia. *N Engl J Med*. Jan 21 2021;384(3):252-260. doi:10.1056/NEJMoa2031054
11. Biasco L, Pellin D, Scala S, et al. In Vivo Tracking of Human Hematopoiesis Reveals Patterns of Clonal Dynamics during Early and Steady-State Reconstitution Phases. *Cell Stem Cell*. 2016/07/07/ 2016;19(1):107-119. doi:<https://doi.org/10.1016/j.stem.2016.04.016>
12. Petrillo C, Thorne LG, Unali G, et al. Cyclosporine H Overcomes Innate Immune Restrictions to Improve Lentiviral Transduction and Gene Editing In Human Hematopoietic Stem Cells. *Cell Stem Cell*. Dec 6 2018;23(6):820-832.e9. doi:10.1016/j.stem.2018.10.008
13. Lee B-C, Lozano RJ, Dunbar CE. Understanding and overcoming adverse consequences of genome editing on hematopoietic stem and progenitor cells. *Molecular Therapy*. 2021/11/03/ 2021;29(11):3205-3218. doi:<https://doi.org/10.1016/j.ymthe.2021.09.001>
14. Tajer P, Canté-Barrett K, Naber BAE, et al. IL3 Has a Detrimental Effect on Hematopoietic Stem Cell Self-Renewal in Transplantation Settings. *Int J Mol Sci*. Oct 22 2022;23(21)doi:10.3390/ijms232112736
15. Fares I, Chagraoui J, Gareau Y, et al. Cord blood expansion. Pyrimidoindole derivatives are agonists of human hematopoietic stem cell self-renewal. *Science*. Sep 19 2014;345(6203):1509-12. doi:10.1126/science.1256337

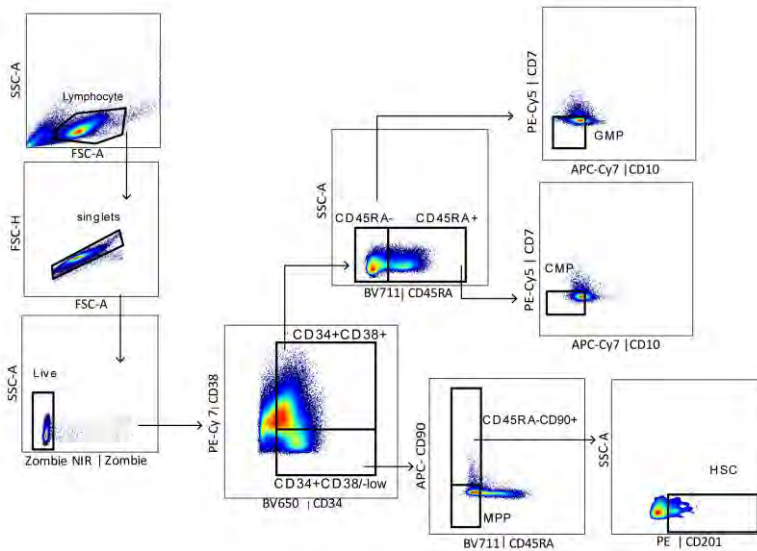
16. Boitano AE, Wang J, Romeo R, et al. Aryl hydrocarbon receptor antagonists promote the expansion of human hematopoietic stem cells. *Science*. Sep 10 2010;329(5997):1345-8. doi:10.1126/science.1191536
17. Sakurai M, Ishitsuka K, Ito R, et al. Chemically defined cytokine-free expansion of human haematopoietic stem cells. *Nature*. 2023/03/01 2023;615(7950):127-133. doi:10.1038/s41586-023-05739-9
18. Rodrigues CP, Shvedunova M, Akhtar A. Epigenetic Regulators as the Gatekeepers of Hematopoiesis. *Trends Genet*. Oct 21 2020;doi:10.1016/j.tig.2020.09.015
19. Hua P, Hester J, Adigbli G, et al. The BET inhibitor CPI203 promotes ex vivo expansion of cord blood long-term repopulating HSCs and megakaryocytes. *Blood*. 2020;136(21):2410-2415. doi:10.1182/blood.2020005357
20. Hua P, Kronsteiner B, van der Garde M, et al. Single-cell assessment of transcriptome alterations induced by Scriptaid in early differentiated human haematopoietic progenitors during ex vivo expansion. *Scientific Reports*. 2019/03/28 2019;9(1):5300. doi:10.1038/s41598-019-41803-z
21. Zimran E, Papa L, Djedaini M, Patel A, Iancu-Rubin C, Hoffman R. Expansion and preservation of the functional activity of adult hematopoietic stem cells cultured ex vivo with a histone deacetylase inhibitor. *Stem Cells Transl Med*. Apr 2020;9(4):531-542. doi:10.1002/sctm.19-0199
22. Chaurasia P, Gajzer D, Feldman M, Hoffman R. Histone Deacetylase Inhibitors Promote the Ex Vivo Expansion of Cord Blood CD34+ Cells in Serum Free Cultures Accompanied by the Upregulation of Pluripotency Genes. *Blood*. 2012;120(21):345-345. doi:10.1182/blood.V120.21.345.345
23. Milhem M, Mahmud N, Lavelle D, et al. Modification of hematopoietic stem cell fate by 5aza 2'deoxyctidine and trichostatin A. *Blood*. 2004;103(11):4102-4110. doi:10.1182/blood-2003-07-2431
24. Estoppey D, Schutzius G, Kolter C, et al. Genome-wide CRISPR-Cas9 screens identify mechanisms of BET bromodomain inhibitor sensitivity. *iScience*. Nov 19 2021;24(11):103323. doi:10.1016/j.isci.2021.103323
25. Venugopal B, Baird R, Kristeleit RS, et al. A Phase I Study of Quisinostat (JNJ-26481585), an Oral Hydroxamate Histone Deacetylase Inhibitor with Evidence of Target Modulation and Antitumor Activity, in Patients with Advanced Solid Tumors. *Clinical Cancer Research*. 2013;19(15):4262-4272. doi:10.1158/1078-0432.Ccr-13-0312
26. Child F, Ortiz-Romero PL, Alvarez R, et al. Phase II multicentre trial of oral quisinostat, a histone deacetylase inhibitor, in patients with previously treated stage IB-IVA mycosis fungoides/Sézary syndrome. *Br J Dermatol*. Jul 2016;175(1):80-8. doi:10.1111/bjd.14427
27. Venugopal B, Baird R, Kristeleit RS, et al. A phase I study of quisinostat (JNJ-26481585), an oral hydroxamate histone deacetylase inhibitor with evidence of target modulation and antitumor activity, in patients with advanced solid tumors. *Clin Cancer Res*. Aug 1 2013;19(15):4262-72. doi:10.1158/1078-0432.Ccr-13-0312
28. Morales Torres C, Wu MY, Hobor S, et al. Selective inhibition of cancer cell self-renewal through a Quisinostat-histone H1.0 axis. *Nat Commun*. Apr 14 2020;11(1):1792. doi:10.1038/s41467-020-15615-z
29. Hao Y, Hao S, Andersen-Nissen E, et al. Integrated analysis of multimodal single-cell data. *Cell*. Jun 24 2021;184(13):3573-3587.e29. doi:10.1016/j.cell.2021.04.048

30. McGinnis CS, Murrow LM, Gartner ZJ. DoubletFinder: Doublet Detection in Single-Cell RNA Sequencing Data Using Artificial Nearest Neighbors. *Cell Syst.* Apr 24 2019;8(4):329-337.e4. doi:10.1016/j.cels.2019.03.003
31. Zappia L, Oshlack A. Clustering trees: a visualization for evaluating clusterings at multiple resolutions. *GigaScience.* 2018;7(7)doi:10.1093/gigascience/giy083
32. Dong G, Xu X, Li Y, et al. Stemness-related genes revealed by single-cell profiling of naïve and stimulated human CD34(+) cells from CB and mPB. *Clin Transl Med.* Jan 2023;13(1):e1175. doi:10.1002/ctm2.1175
33. Finak G, McDavid A, Yajima M, et al. MAST: a flexible statistical framework for assessing transcriptional changes and characterizing heterogeneity in single-cell RNA sequencing data. *Genome Biology.* 2015/12/10 2015;16(1):278. doi:10.1186/s13059-015-0844-5
34. Yu G, Wang LG, Han Y, He QY. clusterProfiler: an R package for comparing biological themes among gene clusters. *OmicS.* May 2012;16(5):284-7. doi:10.1089/omi.2011.0118
35. Chun P. Histone deacetylase inhibitors in hematological malignancies and solid tumors. *Archives of Pharmacal Research.* 2015/06/01 2015;38(6):933-949. doi:10.1007/s12272-015-0571-1
36. Doroshow DB, Eder JP, LoRusso PM. BET inhibitors: a novel epigenetic approach. *Annals of Oncology.* 2017/08/01/ 2017;28(8):1776-1787. doi:<https://doi.org/10.1093/annonc/mdx157>
37. Heffner GC, Bonner M, Christiansen L, et al. Prostaglandin E2 Increases Lentiviral Vector Transduction Efficiency of Adult Human Hematopoietic Stem and Progenitor Cells. *Molecular Therapy.* 2018/01/03/ 2018;26(1):320-328. doi:<https://doi.org/10.1016/j.ymthe.2017.09.025>
38. Jang Y, Kim Y-S, Wielgosz MM, et al. Optimizing lentiviral vector transduction of hematopoietic stem cells for gene therapy. *Gene Therapy.* 2020/12/01 2020;27(12):545-556. doi:10.1038/s41434-020-0150-z
39. Staal FJ, Baum C, Cowan C, et al. Stem cell self-renewal: lessons from bone marrow, gut and iPS toward clinical applications. *Leukemia.* Jul 2011;25(7):1095-102. doi:10.1038/leu.2011.52
40. Nagai Y, Garrett KP, Ohta S, et al. Toll-like receptors on hematopoietic progenitor cells stimulate innate immune system replenishment. *Immunity.* Jun 2006;24(6):801-812. doi:10.1016/j.immuni.2006.04.008
41. Burleigh K, Maltbaek JH, Cambier S, et al. Human DNA-PK activates a STING-independent DNA sensing pathway. *Sci Immunol.* Jan 24 2020;5(43)doi:10.1126/sciimmunol.aba4219
42. Hemmi H, Takeuchi O, Kawai T, et al. A Toll-like receptor recognizes bacterial DNA. *Nature.* Dec 7 2000;408(6813):740-5. doi:10.1038/35047123
43. Piras F, Riba M, Petrillo C, et al. Lentiviral vectors escape innate sensing but trigger p53 in human hematopoietic stem and progenitor cells. *EMBO Molecular Medicine.* 2017;9(9):1198-1211. doi:<https://doi.org/10.15252/emmm.201707922>
44. Passegué E, Ernst P. IFN- α wakes up sleeping hematopoietic stem cells. *Nat Med.* Jun 2009;15(6):612-3. doi:10.1038/nm0609-612
45. de Bruin AM, Demirel Ö, Hooibrink B, Brandts CH, Nolte MA. Interferon- γ impairs proliferation of hematopoietic stem cells in mice. *Blood.* May 2 2013;121(18):3578-85. doi:10.1182/blood-2012-05-432906

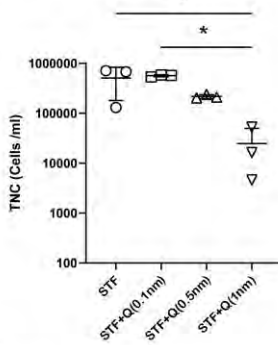
46. Fox T, Bueren J, Candotti F, et al. Access to gene therapy for rare diseases when commercialization is not fit for purpose. *Nat Med*. Mar 2023;29(3):518-519. doi:10.1038/s41591-023-02208-8

Supplementary Material

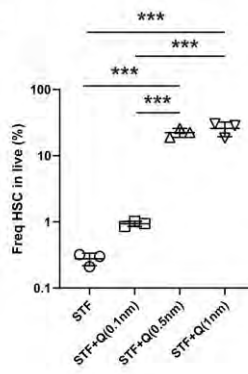
A)



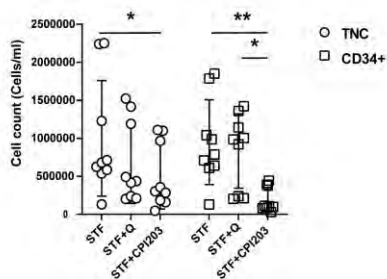
B)



C)



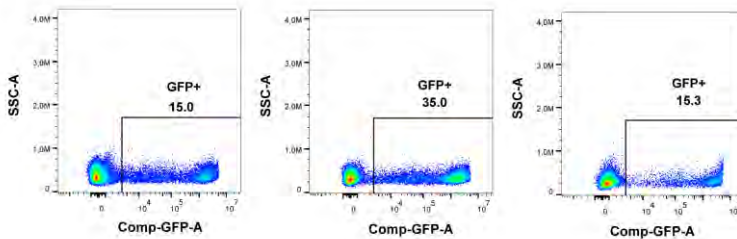
D)



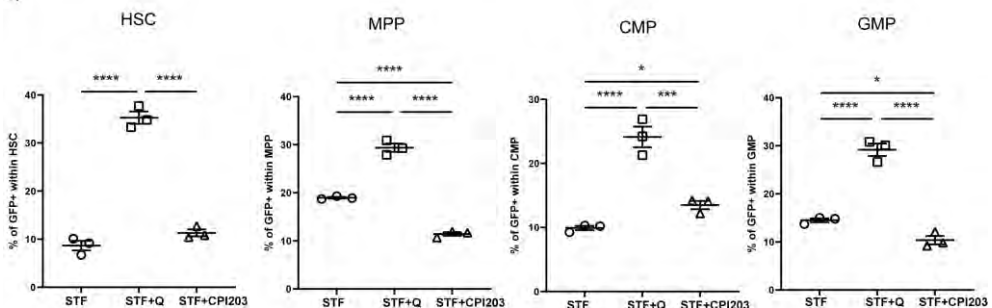
Supplementary Figure 1. Ex vivo expansion of HSPCs. A) Representative gating strategy for phenotypic analysis of HSPCs. B) Total nucleated cell count (TNC) after 4-day culture in presence of different concentration of Quisinostat (n=3, Mean±SD). C) Frequency of HSC after 4-day culture in different concentration of Quisinostat (n=3, Mean±SD). D) TNC and CD34⁺ cell

count after 4 days of expansion in indicated culture condition (n=9, Mean±SD). Significant statistical was determined by two-way anova with multiple comparison * $p < 0.05$, ** $p < 0.01$, *** $p < 0.001$).

A)

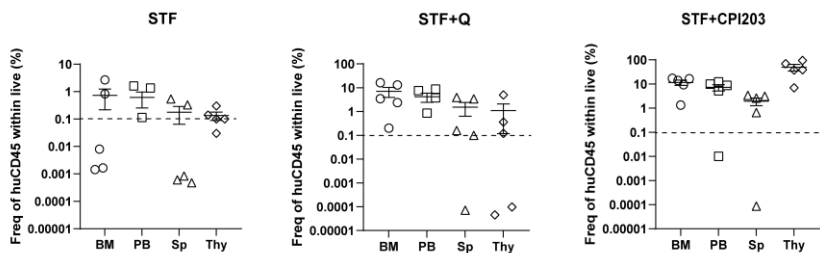


B)



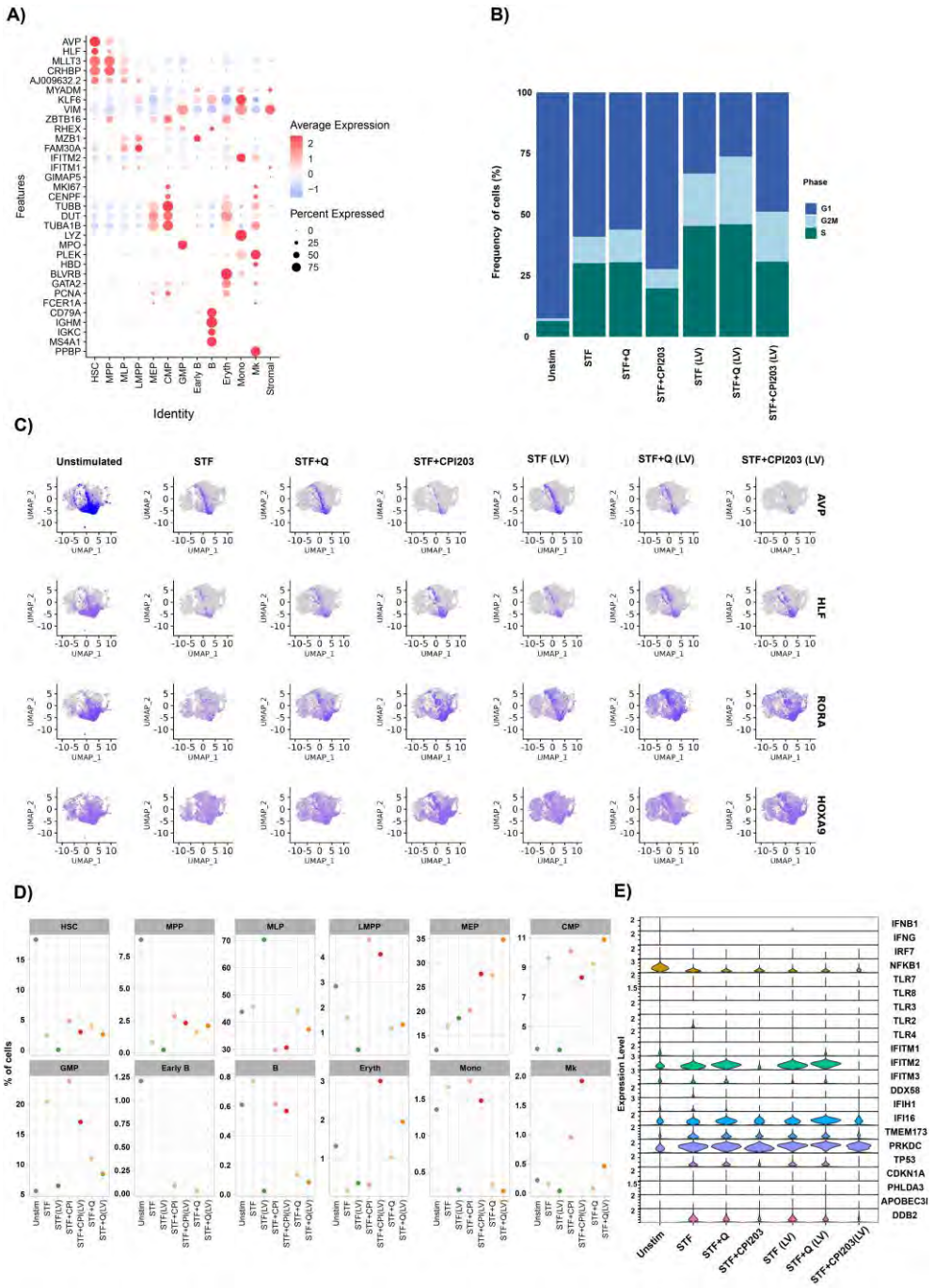
Supplementary Figure 2. LV transduction efficiency in vitro. A) Representative FACS plots displaying GFP expression in live cells, 4 days post transduction. B) Frequency of GFP⁺ in different population of HSC, MPP, CMP and GMP (n=3, Mean±SD, * $p < 0.05$, ** $p < 0.001$, *** $p < 0.0001$). Statistical significance was calculated by two-way anova with multiple comparison)

A)



Supplementary Figure 3. Human engraftment in organs from primary transplanted NSG mice.

A) Frequency of huCD45⁺ in different organs at week 20 post transplantation.



Supplementary Figure 4. Single cell transcriptome of human HSPCs. A) Expression of key marker genes in each cell population (Marker gene set was adopted from *Dong et al*). B) Stacked bar plot showing cell cycle analysis C) Feature plots showing HSC signature genes

expression per condition. D) Plots displaying frequency of different population in indicated conditions. E) Expression of genes inducing interferon response .

Table 2. List of antibodies used for flow cytometry.

Name	Fluoro-chrome	Clone	Source
hCD1a	APC	HI149	BD Biosciences
hCD3	BV786	SK7	BD Biosciences
hCD4	BUV805	SK3	BD Biosciences
hCD5	BV480	UCHT2	BD Biosciences
hCD7	Pe-Cy5	CD7-6B7	Biolegend
hCD8	BV650	RPA-T8	Biolegend
hCD8	BUV496	RPA-T8	BD Biosciences
hCD10	APC-Cy7	HI10a	Biolegend
hCD13	Percp-Cy5.5	WM15	BD Biosciences
hCD19	PE-Cy7	HIB19	Invitrogen
hCD19	BV421	HIB19	Biolegend
hCD20	BV570	2H7	Biolegend
hCD33	Percp-Cy5.5	WM53	BD Biosciences
hCD34	Pe-CF594	581	BD Biosciences
hCD34	BV650	561	Biolegend
hCD38	Pe-Cy7	HIT2	Biolegend
hCD41	BV421	HIP8	Biolegend
hCD45	V450	HI30	BD Biosciences

hCD45RA	BV711	HI100	Biolegend
hCD45RA	BV510	HI100	BD Biosciences
hCD49f	PerCP-ef710	ebioGoH3	Invitrogen
hCD56	PE-Cy5	B159	BD Biosciences
hCD56	APC-Cy7	HCD-56	Biolegend
hCD62L	BV605	DREG-56	BD Biosciences
hCD71	AF700	M-A712	BD Biosciences
hCD90	APC	5 e10	Biolegend
hCD201	PE	RCR-401	Biolegend
hlgM	BV650	MHM-88	BD Biosciences
hlgD	BV480	IA6-2	BD Biosciences
hTCRgd	BV510	11F2	BD Biosciences
hTCRab	PE	MHM-88	BD Biosciences
mCD45	FITC	30-F11	BD Biosciences
Zombie NIR	NIR	-	Biolegend

